SIF2004 Structural Integrity and Fracture. http://eprint.uq.edu.au/archive/00000836

Implementation Of The Local Symmetry Criterion For Crack-Growth Simulations

Matthew Tilbrook* and Mark Hoffman
School of Materials Science & Engineering, University of New South Wales, Sydney, NSW 2052

ABSTRACT: The local symmetry criterion predicts that cracks under mixed-mode loading will deflect so that the local Mode II stress intensity factor, k_{II}, is zero. An efficient approach is presented for its implementation in finite element simulations of crack propagation, based on the observed linearity of k_{II} over a wide range of deflection angles. This linearity is explained by expressing k_{II}, for the kinked crack, in terms of the global stress intensity factors, K_I and K_{II}, and parallel T-stress, σ_T, for the original straight crack. Deflection angles and crack paths obtained agreed with those obtained using a more cautious search algorithm, and with other deflection criteria. This has been particularly applicable to crack-growth simulations in graded materials, where elastic asymmetry results in mixed-mode loading.

1 INTRODUCTION

Cracks frequently experience mixed-mode loading which causes them to deflect and curve. This influences crack propagation rate and, therefore, remaining life and structural integrity. Examples include cracks in complex-shaped components with highly asymmetric stress distribution, such as rotors and flanges [Miranda *et al*., 2003], and in heterogeneous material structures such as interfaces [Rice, 1988] or functionally graded materials (FGMs) [Gu and Asaro, 1997].

Deflection criteria for cracks under mixed-mode loading have received considerable attention [Qian and Fatemi, 1996]. For example, the maximum tangential stress (MTS) criterion [Erdogan and Sih, 1963] predicts that cracks extend in the direction of maximum crack-tip tangential stress. This is calculated by expressing the crack-tip stress distribution in terms of the stress intensity factors (SIFs) for the original crack, K_I and K_{II}, so that the propagation direction, θ_M, may be determined directly from crack-tip mode-mixity, $\Psi = \tan^{-1}(K_{II}/K_I)$:

$$\tan\left(\frac{\theta_M}{2}\right) = \frac{2 - 2\sqrt{1 + 8\tan^2\Psi}}{8\tan\Psi} \qquad (1)$$

Certain other criteria require a small test-kink to be extended from the crack-tip at angle, θ, which is varied to enable calculation of the optimum kink angle, $\theta = \theta_K$, in which, for example, the mechanical energy release rate, G, is maximised [Nuismer, 1975] or crack-tip loading is symmetrical [Goldstein and Salganik, 1974]. The latter, known as the local symmetry or $k_{II} = 0$ criterion, assumes that cracks will always propagate in the Mode I direction, so that k_{II}, the Mode II SIF for the kink, is zero. This criterion has been shown to provide accurate predictions [Qian and Fatemi, 1996]. Implementation within a finite-element model involves the extension of a test-kink from the crack-tip, whose direction is varied to attain a minimum for k_{II}. The successive deletion and remeshing that this necessitates extends computation time significantly [Becker *et al*., 2001, Tilbrook *et al*., 2004].

Investigating the local symmetry criterion for use in simulations of cracks in graded materials, it was observed that the variation in Mode II SIF, k_{II}, with test-kink direction is approximately linear over a wide range of angles. This linearity was utilised in an improved algorithm for finding the optimum deflection angle. This paper discusses the linearity of the k_{II} variation and its implementation for application to crack path predictions.

2 STRESS INTENSITY FACTORS FOR KINKED CRACKS

For an infinitesimally small kink extending at an angle, θ, from the tip of an existing crack, as in Figure 1(b), the stress field acting on the kink may be assumed equivalent to that around the main crack in the absence of the kink, as in Figure 1(a) [Anderson, 1995]. Hence, SIFs at the kink-tip are:

$$k_I(\theta) = C_{11}K_I + C_{12}K_{II} + A_1T\sqrt{r_c} \qquad k_{II}(\theta) = C_{21}K_I + C_{22}K_{II} + A_2T\sqrt{r_c} \qquad (2a,b)$$

where C_{ij} and A_i are angular functions given by Palaniswamy and Knauss [1978] and r_c, related to process zone size [Smith *et al.*, 2001], is equal to the kink-length. The full expression for $k_{II}(\theta)$ is:

$$k_{II}(\theta) = \frac{1}{4}[\sin\left(\frac{\theta}{2}\right) + \sin\left(\frac{3\theta}{2}\right)]K_I + \frac{1}{4}[\cos\left(\frac{\theta}{2}\right) + 3\cos\left(\frac{3\theta}{2}\right)]K_{II} + \sin(2\theta)\sqrt{\frac{\pi r_c}{2}}T \qquad (3)$$

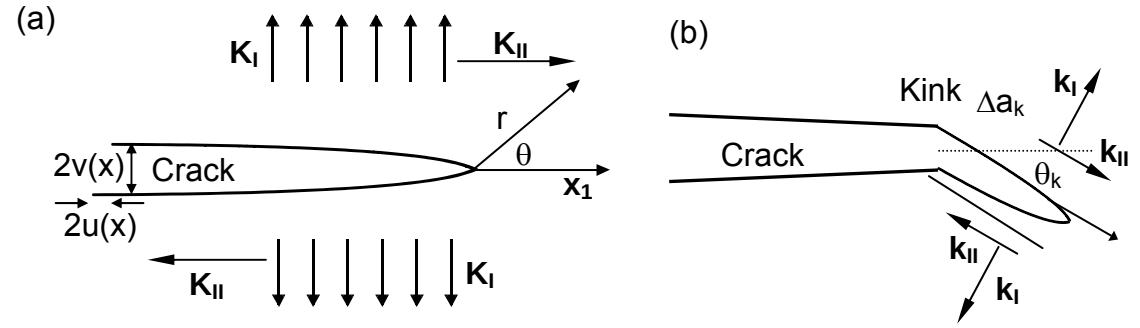

Figure 1. Schematic of crack-tip (a) before and (b) after kinking has occurred.

The case of $r \to 0$, where the T-stress does not influence k_{II}, is considered first. The effect of T-stress on $k_{II}(\theta)$ will be addressed subsequently. The trigonometric functions in Equation 3 may be expressed as Taylor series expansions, around $\theta = \theta_M$, the deflection angle given by the MTS criterion:

$$\text{ie. } \sin\left(\frac{\theta}{2}\right) = \sin\left(\frac{\theta_M}{2}\right) + \frac{1}{2}\cos\left(\frac{\theta_M}{2}\right)(\theta-\theta_M) - \frac{1}{8}\sin\left(\frac{\theta_M}{2}\right)(\theta-\theta_M)^2 - \frac{1}{48}\cos\left(\frac{\theta_M}{2}\right)(\theta-\theta_M)^3 + \ldots \quad (4)$$

The value for θ_M may be determined from Equation 1, or from Equation 3 for $k_{II}(\theta) = T = 0$. Using such series expansions, $k_{II}(\theta)$ may be expressed as a series of terms, $k_{II}^{(n)}(\theta)$, where n is the order in θ:

$$k_{II}(\theta) = k_{II}^{(0)}(\theta) + k_{II}^{(1)}(\theta) + k_{II}^{(2)}(\theta) + k_{II}^{(3)}(\theta) + k_{II}^{(4)}(\theta) + \ldots \qquad (5)$$

The initial, zeroth-order, term is equal to zero, due to the $k_{II}(\theta) = 0$ criterion. The first-order term is

$$k_{II}^{(1)}(\theta) = \frac{K_I}{8}\left(\cos\left(\frac{\theta_M}{2}\right) + 3\cos\left(\frac{3\theta_M}{2}\right)\right)(\theta-\theta_M) - \frac{K_{II}}{8}\left(\sin\left(\frac{\theta_M}{2}\right) + 9\sin\left(\frac{3\theta_M}{2}\right)\right)(\theta-\theta_M) \qquad (6)$$

This is non-zero and is linear in $(\theta-\theta_M)$. The second-order term is:

$$k_{II}^{(2)}(\theta) = \frac{-K_I}{32}\left(\sin\left(\frac{\theta_M}{2}\right) + 9\sin\left(\frac{3\theta_M}{2}\right)\right)(\theta-\theta_M)^2 - \frac{K_{II}}{32}\left(\cos\left(\frac{\theta_M}{2}\right) + 9\cos\left(\frac{3\theta_M}{2}\right)\right)(\theta-\theta_M)^2 \qquad (7)$$

As the derivatives of sine and cosine are cyclic, a dominant part of this expression is proportional to $k_{II}(\theta_M)$, and hence approaches zero as θ approaches θ_M. Similarly the fourth-order term, and all subsequent even terms, will undergo partial cancellation, reducing the magnitude of the symmetric component of the $k_{II}(\theta_M)$ variation. For angles within 30° (~0.5 rad) of θ_M, the increase in power of $(\theta - \theta_M)$ leads to significant diminishing of the higher order terms. The third term, for example, has a dominant part which is proportional to, but much smaller than, the first term:

$$k_{II}^{(3)}(\theta) = \frac{-K_I}{196}\left(\cos\left(\frac{\theta_M}{2}\right) + 27\cos\left(\frac{3\theta_M}{2}\right)\right)(\theta-\theta_M)^3 + \frac{K_{II}}{196}\left(\sin\left(\frac{\theta_M}{2}\right) + 81\sin\left(\frac{3\theta_M}{2}\right)\right)(\theta-\theta_M)^3 \quad (8)$$

The remaining part will also be small, and will partially cancel with the remainder from the second term. Consequently, the dominant linear behaviour may be explained by the partial cancellation of the even terms, resulting from the condition that $k_{II}^{(0)}(\theta)$ is close to zero. Accordingly, the linear term (Equation 6) may be used as an approximation for the $k_{II}(\theta)$.

The variation of $k_{II}^{(T)}$, the T-stress contribution to k_{II}, with angle is not linear [Smith *et al.*, 2001]:

$$k_{II}^{(T)}(\theta) = \sin(2\theta)\sqrt{\frac{\pi r_c}{2}}T \approx T\sqrt{\frac{\pi r_c}{2}}\left[\sin(2\theta_M) + 2\cos(2\theta_M)(\theta - \theta_M) - 2\sin(2\theta_M)(\theta - \theta_M)^2\right] \quad (9)$$

Over the relevant range of angles however, the variation in $k_{II}^{(T)}$ is sufficiently small that the non-linear component does not skew results appreciably. Indeed, the series-expansion arguments above can be extended to demonstrate that the T-stress term does not alter the linearity of $k_{II}(\theta)$ significantly.

3 FINITE ELEMENT IMPLEMENTATION

Crack deflection behaviour was investigated with finite element analysis, which was conducted using ANSYS (Version 6.1, ANSYS Inc, Canonsburg, Pennsylvania). The structures were modelled in two dimensions under plane strain conditions using free-meshed isoparametric quadrilateral elements, with quarter-point singularity elements at the crack-tip, as in Tilbrook *et al.* [2004]. Free meshing was utilised, with significant refinement around the crack-tip to ensure solution accuracy. For graded material simulations, the spatial elastic property variation was applied to nodes. SIFs were calculated from nodal crack-opening displacement values near the crack-tip, both before (K_α) and after (k_α) kinking. A small test kink, Δa_K, was extended from the crack-tip at varying angles, and k_{II} was calculated from nodal displacements.

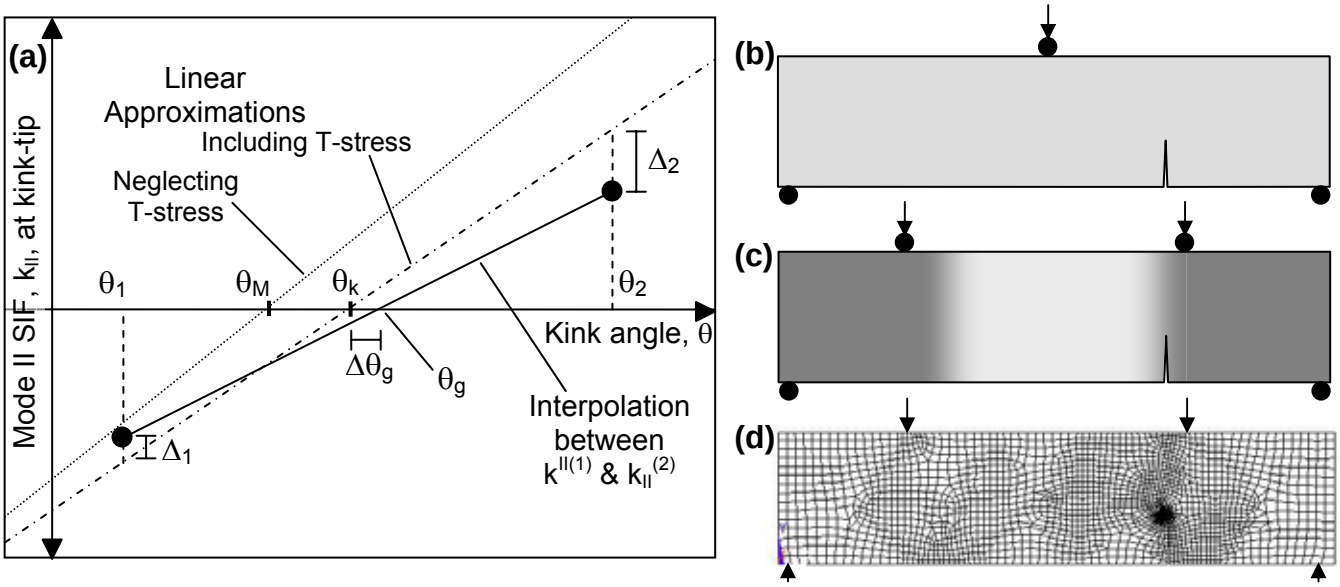

Figure 2. Schematic showing variation of Mode II SIF, k_{II}, with kink angle, θ. Discrepancies, Δ_1 and Δ_2, between actual k_{II} values (●) and linear approximation values, for angles θ_1 and θ_2, resulting in error, $\Delta\theta_g$, in predicted optimum kink angle. Specimen configurations examined: (a) asymmetrically notched homogeneous specimen in three-point bend loading with initially straight crack, and (b) notched graded specimen in four-point bend loading with initially straight crack. A finite element mesh representative of those used for simulations of both specimen types is shown in (c).

Initial upper and lower bounds for the optimum kink angle, θ_{up} and θ_{lo}, were determined from a wide interval around θ_M, the angle predicted by the MTS criterion. The original algorithm was

based on successive 30% reductions of the angular range, until a sufficiently small range was attained.

The linearity of the angular k_{II} variation was exploited in a simple algorithm for finding the optimum kink angle more efficiently. The initial angular bounds, $\theta_1 = \theta_{lo}$ and $\theta_2 = \theta_{up}$, were estimated from θ_M as in the previous method. The optimum angle was estimated directly, from these angles and their corresponding k_{II} values, by interpolation:

$$\theta_g = \theta_1 + (\theta_2 - \theta_1)\frac{k_{II}^{(1)}}{k_{II}^{(2)} - k_{II}^{(1)}} \tag{10}$$

The estimate may be refined by calculating k_{II} for angular bounds closer to the estimated optimum, ie. $\theta = \theta_g \pm \chi$ with χ around 4°, then repeating the interpolation. With this approach, the optimum angle is estimated within ± 0.1° in 4 iterations, compared with 12 or more iterations required for an equivalent estimate with the original approach.

To assess the accuracy of the approach, the error in estimated optimum kink angle was estimated from the intrinsic errors associated with the assumption of linearity. The values of k_{II} for the initial angular bounds will be near the linear values, as in Figure 2(a), with each differing by a small error, Δ_x:

$$k_{II}^{(1)} = m(\theta_1 - \theta_k) + \Delta_1 \qquad k_{II}^{(2)} = m(\theta_2 - \theta_k) + \Delta_2 \tag{11}$$

where m is the linear gradient from $(\theta_1, k_{II}^{(1)})$ to $(\theta_2, k_{II}^{(2)})$. The estimated kink angle, from (10) is:

$$\theta_g = \frac{\theta_1 + \theta_2}{2} - (\theta_2 - \theta_1)\frac{k_{II}^{(2)} + k_{II}^{(1)}}{k_{II}^{(2)} - k_{II}^{(1)}} \tag{12}$$

From (11) and (12), the error in θ_g, the difference between estimated and actual optimum kink angle, is:

$$\Delta\theta_g = \theta_g - \theta_k = -\frac{\Delta_1 + \Delta_2}{2m} + \frac{\Delta_2 - \Delta_1}{2m}\frac{k_{II}^{(2)} + k_{II}^{(1)}}{k_{II}^{(2)} - k_{II}^{(1)}} \tag{13}$$

If the angular bounds were distributed fairly symmetrically about the optimum angle, then $k_{II}^{(2)}$ and $k_{II}^{(1)}$ would be similar in magnitude though opposite in sign, as would be the errors Δ_1 and Δ_2., due to the dominant odd-terms. Accordingly, both terms in (13) will be small, especially so in the refinement step, when the angular bounds are closer to, and more symmetrical about, the optimum angle.

4 CRACK GROWTH SIMULATIONS

The application of the improved algorithm to crack-growth simulations is demonstrated here for two cracked specimen configurations: an asymmetrically-notched homogeneous beam under three-point bend loading, as in Figure 2(b); and an inhomogeneous beam, with longitudinal compositional variation, containing a straight crack under four-point bend loading, as in Figure 2(c). The geometry and meshing for each configuration was very similar. A representative mesh, comprised of approximately 3500 elements, is shown in Figure 2(d).

Values of SIFs and T-stress for the initially unkinked cracks were calculated from nodal stress and displacement values near the crack tip. For the homogeneous specimen, K_I = 1 MPa√m; K_{II} = 0.089 MPa√m; σ_T = 11 MPa; whilst for the graded specimen, K_I = 2.45 MPa√m; K_{II} = 1.15 MPa√m; σ_T = 39 MPa. The results for these are plotted in Figure 4, which compares the FEM results with the predicted variation (Equation 3) and the linear approximation (Equation 6), with and without the inclusion. The high degree of linearity of the k_{II}-θ relationship is apparent. Good agreement may be observed for both specimen configurations.

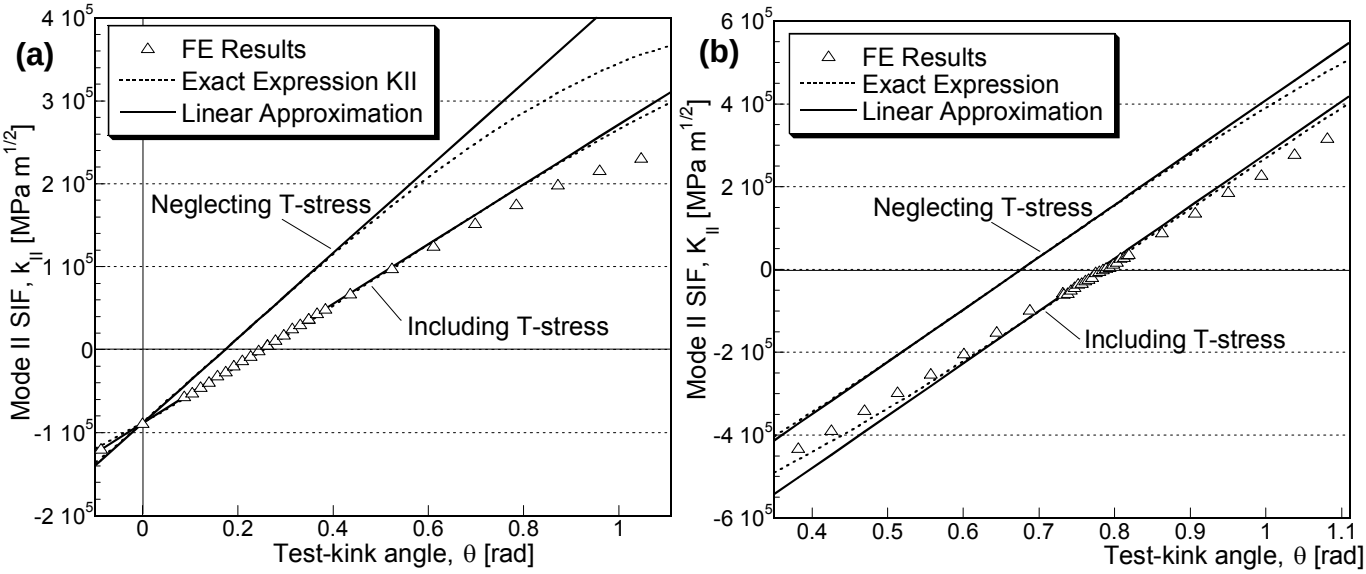

Figure 3. Variation of Mode II stress intensity factor, k_{II}, with kink angle, θ, for initially straight crack in (a) an asymmetrically notched homogeneous specimen under three-point bend loading, and (b) in a notched graded specimen under four-point bend loading. Comparison of predictions, from exact expression and linear approximation, with results from finite element model.

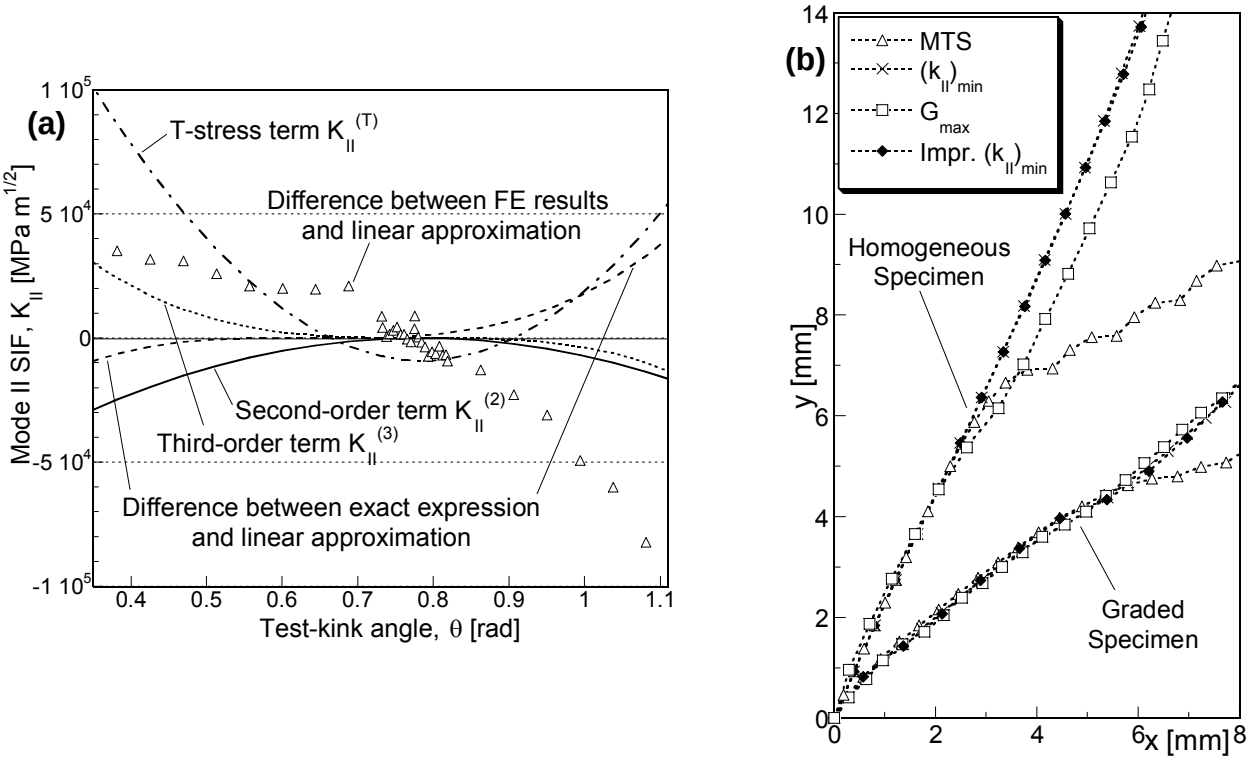

Figure 4. (a) Non-linear component of k_{II} variation. Plot showing discrepancy between linear approximation and exact expression, along with second and third order terms from series expansion, for crack in graded specimen. (b) Predicted propagation paths for cracks in homogeneous and graded specimens. Predictions obtained using the improved algorithm are compared with those obtained using the more rigorous algorithm, with the $(k_{II})_{min}$ and G_{max} criteria.

The non-linear component of the $k_{II}(\theta)$ variation for the graded specimen is illustrated in Figure 4(a). The relative discrepancy between the linear approximation and the exact expression is plotted against θ, and compared with the second and third order terms (Equations 7 and 8), and the T-stress contribution. It may be observed that the relative discrepancy is small, and the higher order terms

have a very minor influence, in the case investigated. This indicates that the use of the linear approximation in estimating optimum deflection angle is valid, though the use of refinement step is recommended.

Crack propagation paths were simulated for both specimen configurations, utilising the improved algorithm. For comparison, simulations were also conducted using the original algorithm with the $(k_{II})_{min}$ criterion and the G_{max} criterion, and using the MTS criterion which does not require a test-kink. Predicted crack paths are shown in Figure 4(b) for both specimen configurations. Clearly there is excellent agreement between results from all approaches, with the only exception being a divergence of the MTS predictions for both specimens later in the crack propagation, due to T-stresses which influence crack path but are not taken into account in MTS predictions [Tilbrook *et al.*, 2004].

5 CONCLUSIONS

1. The variation of Mode II stress intensity factor, k_{II}, at the tip of a kinked crack with the deflection angle of the kink is close to linear, to a very close approximation, over a wide range of deflection angles, and is predominantly antisymmetric about $k_{II} = 0$.
2. This was explained in terms of the expression for Mode II SIF for a small kink, which can be expanded as a series. The linear term, and subsequent odd terms, dominated due to partial cancellation of the even terms.
3. This has been utilised in an algorithm for prediction of optimum deflection angles, which increased the efficiency of crack path simulations significantly without compromising accuracy.

REFERENCES

Anderson TL, Fracture Mechanics: Fundamentals & Applications, CRC Press, Boca Raton, 1995.

Becker, T L Jr, Cannon, R M and Ritchie, R O, Finite crack-kinking and T-stresses in functionally graded materials, *Int. J. Sol. Str.*, **38**, 5545 (2001)

Erdogan F and Sih G C. On the crack extension in plates under plane loading and transverse shear, *J. Basic. Eng. ASME Trans.,* **85**, 519 (1963)

Goldstein, R V and Salganik, R L, Brittle fracture of solids with arbitrary cracks, Int. J. Fract., **10**, 507 (1974).

Gu, P and Asaro, R J, Crack Deflection in Functionally Graded Materials. *Int. J. Sol. Struct.* **34**, 3085 (1997).

Kim, J-H and Paulino G, Finite element evaluation of mixed mode stress intensity factors in functionally graded materials. *Int. J. Numer. Meth. Engng.* **53**, 1903 (2002).

Miranda, A C O, Meggiolaro, M A, Castro, J T P, Martha, L F, Bittencourt, T N, Fatigue life and crack path predictions in generic 2D structural components, *Engng. Fract. Mech.* **70**, 1259 (2003).

Nuismer, R J, An energy release rate criterion for mixed mode fracture, *Int. J. Fract.*, **11**, 245 (1975).

Palaniswamy, K and Knauss, W G, On the problem of crack extension in brittle solids under general loading, *Mechanics Today*, ed. S Nemat-Nasser, **4**, Pergamon Press (1978)

Qian, J and Fatemi, A, Mixed mode fatigue crack growth: literature survey. *Engng. Fract. Mech.* **55**, 969 (1996)

Rice, J R, Elastic Fracture Mechanics Concepts for Interfacial Cracks, *J. Appl. Mech.*, **55**, 98 (1988).

Smith, D J, Ayatollah, M R, Pavier, M J, The role of T-stress in brittle fracture for linear elastic materials under mixed-mode loading. *Fatigue Fract. Engng. Mater. Struct.* **24**, 137–150 (2001)

Tilbrook, M T, Moon, R J, and Hoffman, M, Finite Element Analysis of Crack-Tip Stresses and Crack Propagation in Functionally Graded Materials, *Engng. Fract. Mech.*, submitted (2004)